Acta Crystallographica Section D
Biological Crystallography
ISSN 0907-4449

Structure of thaumatin in a hexagonal space group: comparison of packing contacts in four crystal lattices

Christophe Charron,‡ Richard Giegé and Bernard Lorber*

Département 'Mécanismes et Macromolécules de la Synthèse Protéique et Cristallogenèse' UPR 9002, Institut de Biologie Moléculaire et Cellulaire du CNRS, 15 Rue René Descartes, F-67084 Strasbourg CEDEX, France

‡ Present address: Laboratoire de Cristallographie et Modélisation des Matériaux Minéraux et Biologiques, UMR 7036 du CNRS, Groupe Biocristallographie, Université Henri Poincaré–Nancy I, BP 239, F-54506 Vandoeuvre-lès-Nancy, France.

Correspondence e-mail: b.lorber@ibmc.u-strasbg.fr

Received 6 August 2003
Accepted 9 October 2003

PDB Reference: thaumatin, 1pp3, r1pp3sf.

The intensely sweet protein thaumatin has been crystallized in a hexagonal lattice after a temperature shift from 293 to 277 K. The structure of the protein in the new crystal was solved at 1.6 Å resolution. The protein fold is identical to that found in three other crystal forms grown in the presence of crystallizing agents of differing chemical natures. The proportions of lattice interactions involving hydrogen bonds, hydrophobic or ionic groups differ greatly from one form to another. Moreover, the distribution of acidic and basic residues taking part in contacts also varies. The hexagonal packing is characterized by the presence of channels parallel to the *c* axis that are so wide that protein molecules can diffuse through them.

1. Introduction

Crystals are a prerequisite for any crystallographic study. In the case of biomacromolecules, nucleation and subsequent growth of suitable single crystals often only occurs in a narrow range of conditions, *i.e.* in one or a few solutions having well defined compositions. In order to cover a broad set of conditions during an initial search, most experimenters employ matrices that test parameters such as solvent, precipitant, pH, temperature and chemical additives. For each parameter, the level, nature or concentration is varied in the presence of a given amount of pure and homogenous macromolecule (Ducruix & Giegé, 1999; McPherson, 1999).

A new matrix was designed in-house in which some ingredients are purposefully common to all conditions. When it was tested with the naturally sweet monomeric protein thaumatin (M_r = 22 400), a hexagonal crystal form was found that diffracted X-rays to high resolution. The latter adds to the three forms of different habits and space groups ($P4_12_12$, $P2_12_12_1$ and $C2$) for which complete three-dimensional structures are known (Ko *et al.*, 1994). Here, we report the structure of this novel crystal form and compare the amino-acid residues and chemical groups that are involved in the packing of thaumatin molecules in four crystallization conditions. Similarities to and differences from other proteins give an insight into protein crystallogenesis. In relation to this, the method of exploring the space of possible crystallization conditions is discussed.

2. Materials and methods

2.1. Chemicals and protein crystallization

Solutions were made with ultrapure sterile water containing 0.01%(*m*/*v*) NaN_3 and filtered through membranes of 0.22 µm pore diameter (Ultrafree-MC, Cat. No. UFC30GV00, Milli-

Table 1
Crystallization conditions and crystal data of different crystal forms of thaumatin.

Space group	$P6_1$	$P4_12_12$†	$P2_12_12_1$‡§	$C2$‡¶
Crystallization				
Protein concentration (mg ml^{-1})	35	35	16	16
Solution composition	0.7 *M* $(NH_4)_2SO_4$, 0.04 *M* $LiSO_4$, 0.04 *M* $MgCl_2$, 6%(*v*/*v*) glycerol, 0.8%(*m*/*v*) PEG 400	0.73 *M* Na tartrate	14%(*m*/*v*) PEG 4000	16%(*m*/*v*) PEG 4000, 0.02 *M* NaCl
Buffer	0.04 *M* Na acetate pH 4.5	0.1 *M* ADA†† pH 6.5	0.08 *M* Tris–HCl pH 8.0	None
Temperature (K)	277	293	296	296
Crystal data				
Unit-cell parameters (Å, °)	$a = b = 144.8$, $c = 47.7$	$a = b = 57.9$, $c = 150.0$	$a = 44.3$, $b = 63.7$, $c = 72.7$	$a = 117.7$, $b = 44.9$, $c = 38.0$, $\beta = 94.0$
Asymmetric unit content	2 monomers	1 monomer	1 monomer	1 monomer
V_M (Å^3 Da^{-1})	3.26	2.83	2.31	2.26
Solvent content (%)	61	55	45	43
Diffraction limit (Å)	1.60	1.36	1.75	2.60

† Charron *et al.* (2002); PDB code 1ly0. ‡ Ko *et al.* (1994); McPherson & Weickmann (1990). § PDB code 1thv. ¶ PDB code 1thu. †† *N*-(2-Acetamido)-2-iminodiacetic acid.

pore). DNase-, RNase- and protease-free glycerol and ACS grade ammonium sulfate were gifts from Acros Organics (Geel, Belgium). PEG 400 was purchased from Hampton Research, lithium sulfate from Fluka, magnesium chloride from Merck and concentrated acetic acid from Prolabo.

Lyophilized thaumatin I from *Thaumatoccus daniellii* (Cat. No. T-7638; Lot 108 F00299) was purchased from Sigma. The protein (SWISS-PROT code P02883, 207 amino acids, M_r = 22 204) was dissolved in water and insoluble material removed by centrifugation at 10 000 rev min^{-1} followed by filtration through a membrane of 0.22 µm pore diameter. The protein concentration was determined from the absorbance at 280 nm using an extinction coefficient of 1.25 for a 1 mg ml^{-1} solution and a 1 cm path length. Crystallization assays were set up at 277 K using the vapour-diffusion method. Hanging drops were prepared manually by mixing one volume (5 µl in the initial search, 10 µl for preparative purposes) of protein solution at 30 mg ml^{-1} with one volume of reservoir solution. The drops were deposited onto organosilane-treated glass cover slips. The reservoir volume was 300 µl in modular plates (Lorber & Cudney, 2002). Once microcrystals were obtained, the conditions were refined by slightly varying the composition of the reservoir solution. To do this, the stock solutions were mixed with water in various proportions.

2.2. X-ray diffraction data collection and structure determination

Diffraction data were collected at 100 K on beamline ID14-2 at the European Synchrotron Radiation Facility (ESRF, Grenoble) with incident radiation at a wavelength of 0.933 Å and a crystal-to-detector distance of 140 mm. Prior to data collection, a suitable crystal was flash-frozen after a 15 s dip in mother liquor containing 30%(*v*/*v*) glycerol. Diffraction patterns were recorded on a Quantum ADSC-Q4 CCD detector by 0.5° oscillations with 5 s exposure times over a range of 130°. Data were indexed and scaled using *XDS* (Kabsch, 1993) and the indexed intensities were converted to structure factors without any σ cutoff.

The structure of thaumatin was solved by molecular replacement in the resolution range 10.0–3.5 Å using the model derived from the $P4_12_12$ crystal form (Charron *et al.*, 2002; PDB code code 1ly0) and the program *AMoRe* (Navaza, 1994). Refinement in the 30–1.60 Å resolution range was performed using the *CNS* package (Brünger *et al.*, 1998) and 7% of the data were selected for $R_{\rm free}$ calculations. During refinement of the initial structure, the whole molecule was treated as a rigid body. This was followed by molecular-dynamics refinement using the simulated-annealing technique. Electron-density maps were calculated to correct and rebuild the model wherever necessary using *O* (Jones *et al.*, 1991). The model was further refined and water molecules were defined using the *CNS* package (Brünger *et al.*, 1998). The stereochemical acceptability of the structure was verified using the program *PROCHECK* (Laskowski *et al.*, 1993).

The neighbours of a thaumatin molecule in a given crystal packing were generated using the program *O* (Jones *et al.*, 1991). The solvent-accessible surface area was estimated using the algorithm of Lee & Richards (1971) implemented in the *CNS* package (Brünger *et al.*, 1998). The solvent-probe radius was set at 1.4 Å. The surface area of a molecule buried by intermolecular interactions was calculated as the difference between the accessible surface area of the molecule *in vacuo* and that in the crystal. The cutoff distance was set at 4.5 Å for crystal contacts.

3. Results

3.1. A novel crystal form for thaumatin

In our hands, using the natural and commercially available product (isoform I), commercial sparse matrices (Jancarik & Kim, 1991) failed to produce an additional crystal form of thaumatin to that which grows in the presence of tartrate ions. For this reason, a simplified sparse matrix was designed based on a compilation of publicly available matrices and covering only 24 conditions. In this set, each of the 24 solutions contains 15%(*v*/*v*) glycerol with 100 m*M* lithium sulfate and 100 m*M* magnesium chloride. The precipitant is a pure salt, a polyethylene glycol, a short-chain alcohol or a mixture of two of them. Four buffering substances explore the pH range 3.5–10. Upon testing this matrix with two thaumatin concentrations

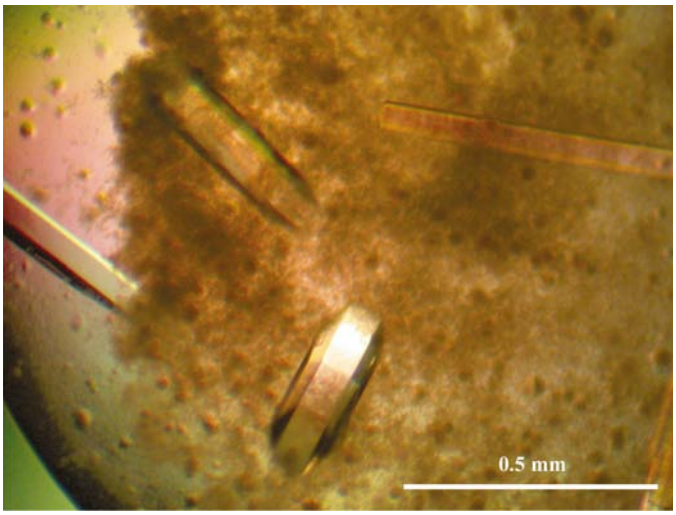

Figure 1
Hexagonal crystals of thaumatin.

(10 and 30 mg ml^{-1}) and at two temperatures (277 and 293 K), a novel crystal form was obtained reproducibly. Crystals of identical hexagonal habit could also be prepared when the assay conditions diverged slightly from the initial conditions (Table 1), *e.g.* with a protein concentration between 10 and 60 mg ml^{-1} or with modified equilibration kinetics after changing either the reservoir volume (from 100 or 200 µl) or the initial temperature (from 293 to 277 K).

Hexagonal rods of up to 0.5 mm in length (thickness $\simeq$ 150 µm; Fig. 1) could be prepared reproducibly in the presence of 0.7 *M* ammonium sulfate, 6%(*v*/*v*) glycerol, 0.8%(*v*/*v*) PEG 400, 40 m*M* lithium sulfate, 40 m*M* magnesium chloride and 40 m*M* sodium acetate adjusted to pH 4.5. A small number of crystals (1–6) per drop repeatedly formed in a milky precipitate after 2–3 weeks when assays were either placed immediately at 277 K or first kept at 293 K and subsequently moved to the final temperature. Attempts to determine a diffusion coefficient by dynamic light-scattering measurements on undersaturated solutions were unsuccessful because the protein strongly aggregates at the lowest protein ($\sim$1 mg ml^{-1}) and crystallizing agent concentrations (*e.g.* a sixfold dilution of the above crystallization medium).

Table 2
Data-collection and refinement statistics for thaumatin in its hexagonal crystal form.

Values in parentheses are for the highest resolution shell.

Crystallization temperature (K)	277
Data-collection temperature (K)	100
Space group	$P6_1$
Unit-cell parameters (Å)	$a = b = 144.8$, $c = 47.7$
Resolution (Å)	1.60 (1.60–1.69)
R_{sym} (%)	7.4 (21.5)
Completeness(%)	97.9 (99.0)
Average $I/\sigma(I)$	17.5
Multiplicity	7.5
Resolution used in refinement (Å)	30.0–1.60
R factor (%)	21.1
R_{free}† (%)	22.3
R.m.s. deviations from ideal	
Bond lengths (Å)	0.006
Bond angles (°)	1.34
No. protein atoms	3104
No. water molecules	377
Average *B* factor (Å^2)	
Protein atoms	18.8
Water molecules	29.7

† 7% of the reflections were used for computing R_{free}.

3.2. Structure of thaumatin in the hexagonal lattice

Crystals belong to space group $P6_1$, with unit-cell parameters $a = b = 144.8$, $c = 44.7$ Å. A total of 555 068 reflections in the resolution range 30–1.60 Å were collected from one

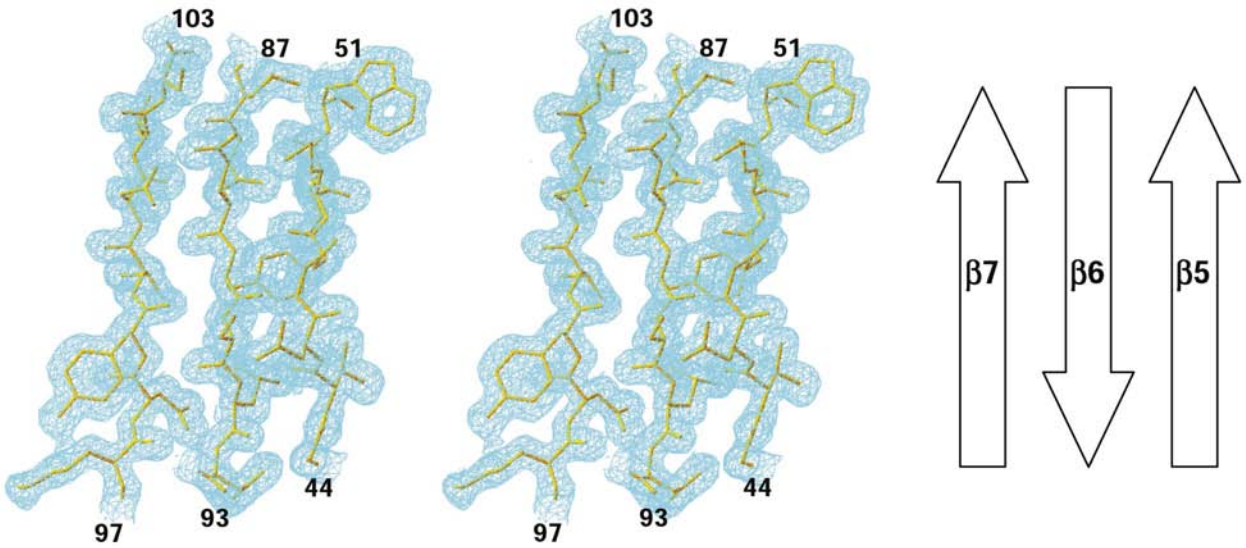

Figure 2
Stereoview of the $2F_o - F_c$ electron-density map (contoured at 1σ) of part of one β-sheet of thaumatin.

Table 3
R.m.s. deviations (Å) between model coordinates of the hexagonal and of the $P4_12_12$, $C2$ and $P2_12_12_1$ crystal forms, respectively.

	C^α	Backbone†	All atoms‡
$P6_1(A)/P6_1(B)$	0.393	0.476	0.828
$P6_1(A)/P4_12_12$	0.725	0.724	1.160
$P6_1(B)/P4_12_12$	0.680	0.714	1.233
$P6_1(A)/C2$	0.683	0.730	1.256
$P6_1(B)/C2$	0.667	0.732	1.371
$P6_1(A)/P2_12_12_1$	0.551	0.557	1.164
$P6_1(B)/P2_12_12_1$	0.583	0.600	1.208

† Including C^α, N, C and O atoms. ‡ For residue 46, only the atoms in common were compared.

crystal at the synchrotron beamline. They were reduced to 74 168 unique reflections. Overall, the data set had an $R_{\rm sym}$ of 7.4% on intensities ($R_{\rm sym} = \sum |I - \langle I\rangle| / \sum I$) and was 97.9% complete (Table 2). The alternative space group $P6_122$ was eliminated because of the high $R_{\rm sym}$ value (46%). Assuming the presence of two molecules of thaumatin in the asymmetric unit, the packing density $V_{\rm M}$ is 3.26 Å^3 Da^{-1} and the solvent content is 61%. These values are in good agreement with those of other proteins (Matthews, 1968).

Molecular replacement was performed using a model derived from the $P4_12_12$ crystal form (Charron *et al.*, 2002). The rotation function calculated with a 30 Å integration radius had two major peaks with heights of 13.5 and 11.5 r.m.s. The orientations corresponding to the first two peaks were subsequently used in the calculation of the translation function in space group $P6_1$. They gave one major peak for each orientation (correlation C = 28.1%, R factor = 47.2% and C = 29.3%, R factor = 46.9%, respectively). Calculation of the translation function with two molecules in the asymmetric unit gave one major peak (C = 49.3% and R factor = 40.4%). The second peak had a correlation of only 20.3%.

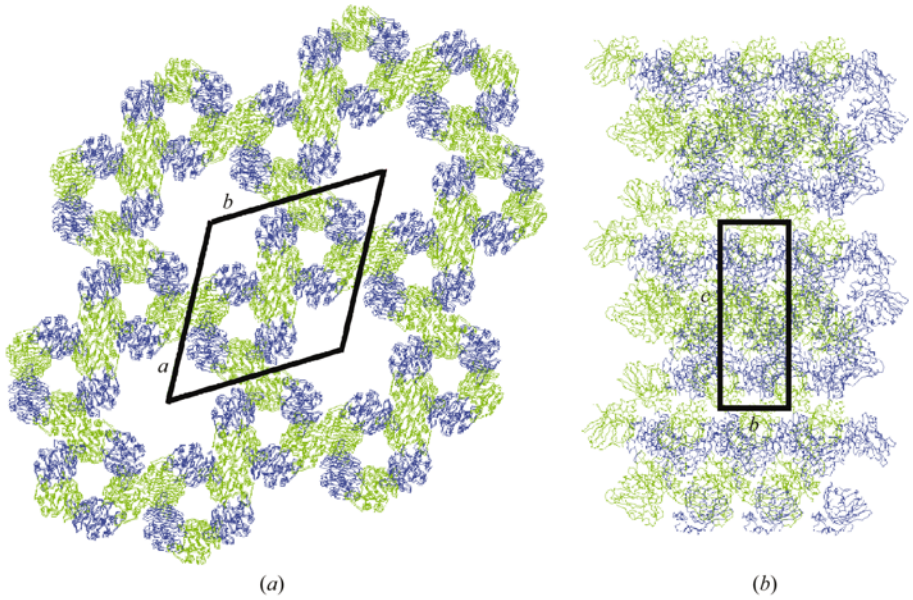

Figure 3
Packing of thaumatin molecules in the hexagonal crystalline lattice. The views of the unit-cell contents are along (*a*) the *c* axis and (*b*) the *b* axis of the crystal lattice. Monomer *A* is displayed in green.

The structure of the protein was refined to a final R factor of 21.1% and an $R_{\rm free}$ of 22.3% (Table 2). Part of the density map corresponding to the β-sheet is displayed in Fig. 2. The asymmetric unit contains two monomers of thaumatin (207 residues) and 377 molecules of water. About 80% of these water molecules are directly in contact with the protein. Of these, 40% interact with side-chain atoms, of which half belong to neutral residues. The conformations of both thaumatin molecules are very similar: superimposition of the backbone atoms resulted in a r.m.s. deviation of only 0.476 Å. The average value of the B factor is 18.8 Å^2 for protein atoms and of 29.7 Å^2 for water molecules.

Table 3 lists the differences in r.m.s. deviation between the coordinates of the model refined in the hexagonal lattice and those of the model in three other space groups. These deviations are similar to the overall deviations between the models corresponding to the $C2$, $P2_12_12_1$ and $P4_12_12$ space groups (Ko *et al.*, 1994). Indeed, the polypeptide backbone is virtually unaltered.

The packing of thaumatin monomers in the hexagonal crystal is shown in Fig. 3. Large channels measuring 80 Å in diameter and smaller ones with a diameter of 25 Å run parallel to the *c* axis and go right through the crystal. In contrast, the packing is more compact along the *a* and *b* axes.

3.3. Packing contacts in four crystal lattices

Table 4 lists the amino-acid residues located within each area of contact that take part in particular lattice interactions (such as hydrogen bonds, ionic and hydrophobic interactions). Half of these interactions involve hydrogen bonds and about one quarter occur *via* ionic bonds. Hydrophobic interactions are even scarcer. The surface buried by the various contacts ranges from 150 to 1000 Å^2. For a single thaumatin molecule, the buried surface amounts to ~2550 Å^2. The monomers *A* and *B* share four contacts. Each *A* monomer also makes two specific contacts with other *A* monomers. The same holds for contacts between *B* monomers. In the asymmetric unit, monomers *A* and *B* are related by a dyad axis and their contact surface area (when *A* and *B* are in position x, y, z) involves the same residues of each partner (by symmetry). The average surface area that is buried on the *A* and *B* monomers is about the same. *A*–*A* and *B*–*B* contacts represent only a small part of the total number of contacts. Thus, apart from small differences in the nature of the *A*–*A* and *B*–*B* contact areas, the environment of the *A* monomers is roughly similar to that of the *B* monomers.

As shown in Fig. 4, the distribution of charged residues making salt bridges is not homogeneous over the protein

surface. All of them are found in the N-terminal part of the protein and are involved in contacts with two neighbouring molecules. 11 of the 25 residues that are involved in the hexagonal crystal packing also make contacts in other lattices. For instance, Glu35 and Lys187 are involved in salt bridges in the monoclinic lattice, while Arg8, Ser33, Arg82 and Arg119 are found in the tetragonal intermolecular interactions (Ko *et al.*, 1994). In the orthorhombic space group, Arg76 and Tyr95 contribute to crystal packing (Ko *et al.*, 1994). Interestingly, one hydrophobic interaction (Tyr57–Ile65) and one ionic interaction (Asp60–Arg119) from the hexagonal lattice are also found in the monoclinic and tetragonal lattices, respectively.

Table 5 lists the protein surface that is buried upon crystallization in each crystal form. In the hexagonal lattice, each molecule is in contact with six neighbours and the buried surface is ~2550 Å^2. This represents 22.7% of the total solvent-accessible surface of the thaumatin molecule. Interestingly, the number of neighbours does not seem to be correlated with the contact area. Indeed, the protein surface buried upon crystallization is larger in the tetragonal lattice, while the packing valence is 7. By contrast, the orthorhombic lattice shows the lowest buried surface and the highest packing valence.

Table 4
Intermolecular interactions between amino-acid residues and buried surface area in the hexagonal packing.

Only residues taking part in particular lattice interactions within the area of contact are listed. Each monomer *A* has contacts with four *B* monomers and two *A* monomers. Each monomer *B* has four contacts with *A* monomers and two with other *B* monomers.

Contacts between monomers	Interacting residues†	Buried surface area (Å^2)
x, y, z (*A*) ↔ $x, y,$ z (*B*)	Tyr57—Ile65^{HY}, Asp59—Arg82^{i}, Asp60—Arg82^{i}, Ile65—Tyr57^{HY}, Ile65—Ile65^{HY}, Arg82—Asp59^{i}, Arg82—Asp60^{i}	400
x, y, z (*A*) ↔ $x, y, z - 1$ (*B*)	Thr2—Arg76^{H}, Glu4—Arg29^{i}, Arg8—Glu35^{i}, Arg29—Thr38^{H}, Ser36—Thr38^{H}, Arg119—Asp60^{i}	500
x, y, z (*A*) ↔ $1 - y, x - y, z - 2/3$ (*B*)	Phe80—Tyr95^{HY}, Tyr95—Phe0^{HY}, Lys187—Leu185^{H}	1000
x, y, z (*A*) ↔ $2 - x, 1 - y, z - 1/2$ (*B*)	Gly132—Gln30^{H}, Gly132—Asn32^{H}, Ala136—Ser33^{H}	350
x, y, z (*A*) ↔ $2 - x, 1 - y, z - 1/2$ (*A*)	Ala207—Pro141^{H}	150
x, y, z (*A*) ↔ $2 - x, 1 - y, z + 1/2$ (*A*)	Pro141—Ala207^{H}	150
x, y, z (*B*) ↔ $x, y, z - 1$ (*B*)	Arg119—Thr150^{H}, Arg119—Val151^{H}	150
x, y, z (*B*) ↔ $x, y, z + 1$ (*B*)	Thr150—Arg119^{H}, Val151—Arg119^{H}	150

† H, Hydrogen bonds; i, ionic interactions; HY, hydrophobic contacts.

Table 5
Packing contacts in the four crystal forms of thaumatin.

	PDB code	Crystallizing agent	Buried surface area (Å^2)	No. of neighbours†
$P2_12_12_1$	1thv	PEG 4000	2050	10
$C2$	1thu	PEG 4000 + sodium chloride	2100	9
$P6_1$	1pp3	Ammonium sulfate + PEG 400	2200‡	6
$P4_12_12$	1ly0	Sodium tartrate	2480	7

† Thaumatin molecules closer than 4.5 Å are considered to be neighbours. ‡ The molecules *A* and *B* have similar buried surface areas.

4. Discussion and conclusions

4.1. Peculiarities of thaumatin crystal packing

Five distinct crystal forms of thaumatin have been reported since 1975, but it seems that some cannot be made to order using each isoform of the protein. So far, isoform I (having Asn residues at positions 46 and 113) has been crystallized (at neutral pH) either in an orthorhombic space group in the presence of either ammonium sulfate (van der Wel *et al.*, 1975; de Vos *et al.*, 1985) or in a tetragonal space group in the presence of tartrate ions (Sauter *et al.*, 2002). At room temperature, isoforms A (characterized by Asn46 and Asp113) and B (with Lys46 and Asn113) were grown either as orthorhombic or monoclinic crystals in the presence of PEG at neutral to slightly alkaline pH (McPherson & Weickmann, 1990; Ko *et al.*, 1994). At lower temperature and at acidic pH, a mixture of ammonium sulfate and low-molecular-weight PEG (with glycerol, lithium sulfate and magnesium chloride as additives) yielded hexagonal crystals of thaumatin I (Table 1). Viewed down the *c* axis, the internal structure of these crystals resembles bunches of nanotubes or hollow fibres having solvent channels whose cross-section is large enough to permit the diffusion of protein molecules (Fig. 3*a*). It shares some similarity with the recently reported structure of hexagonal ($P6_5$) histone-core octamer crystals (Chantalat *et al.*, 2003).

4.2. Properties of crystal in salt *versus* polyethylene glycol solutions

The four structure models of thaumatin give some clues about how protein–protein interactions vary with the chemical nature of the crystallizing agent. Although the fold of the polypeptide backbone and its side chains are almost identical in all forms, major differences exist at the level of the nature, charge and position of the interacting residues. As can be seen in Table 2, crystals growing in the presence of a salt have a higher solvent content (55–61%) than those grown with PEG (43–45%). The same trend has previously been observed with aspartyl-tRNA synthetase (DRS 1) from *Thermus thermophilus* (Charron *et al.*, 2001).

The buried surface of the thaumatin monomer is 20% greater when the crystallizing agent is a pure salt instead of a pure PEG (Table 5). Independently of the space group, a difference in buried surface area ranging from only 3% to as high as 77% was observed in the case of RNAse (Crosio *et al.*,

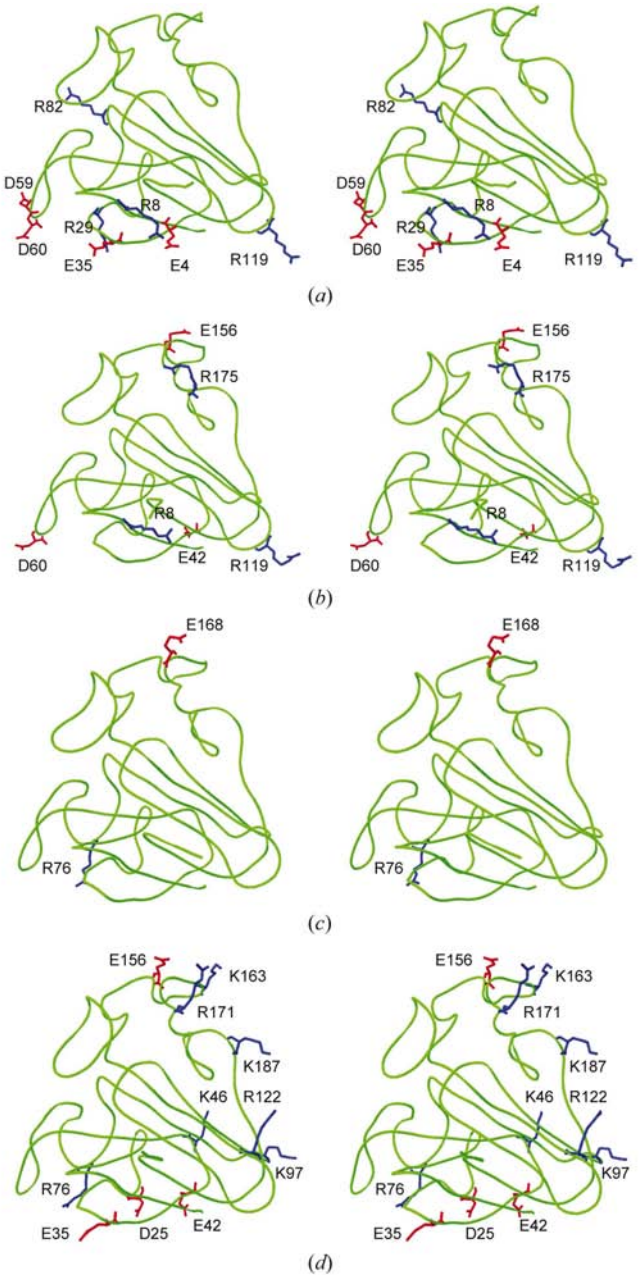

Figure 4
Stereoviews of the distribution of charged residues (alkaline in blue and acidic in red) making salt bridges in thaumatin intermolecular crystal contacts within the (*a*) $P6_1$, (*b*) $P4_12_12$, (*c*) $P2_12_12_1$ and (*d*) $C2$ lattices.

1992) and was over 80% in the case of the above-mentioned synthetase. Surprisingly, the limit of diffraction of the crystals of the three aforementioned proteins grown in pure salt solution is superior to that of those grown in PEG solution. On the other hand, there is apparently no correlation between the crystallization conditions and the number or positions of the thaumatin residues that are involved in ionic interactions (Fig. 4). The effects are probably subtler. Finally, no small molecule is visible in the crystal forms besides a tartrate ion that occupies a key position between three protein monomers in the tetragonal crystal packing (Ko *et al.*, 1994; Sauter *et al.*, 2002).

5. Concluding remarks

The case of thaumatin illustrates how testing a further crystallization condition can yield crystals diffracting to high resolution. It reminds us that the sparse-matrix approach has limits (see, for example, Carter & Carter, 1979; Samudzi *et al.*, 1992; Carter *et al.*, 1994; Cudney *et al.*, 1994; Kingston *et al.*, 1994; Stura *et al.*, 1994; Sedzik & Norinder, 1997; Segelke, 2001). Indeed, its success is highly dependent on the nature of the chemicals that are screened. Therefore, missing conditions that have never been assayed must be identified. Ignorance of the range of conditions under which a given protein is stable, remains monodisperse (*i.e.* unaggregated and not denatured) and can crystallize is the actual obstacle. *A priori*, the way to find the limits of the *N*-dimensional space of conditions that should systematically be explored is to understand the rules of protein stability and those of crystallization. Proteins or viruses that form well diffracting crystals in several solvents (*i.e.* in the presence of crystallizing agents of different chemical natures) are good candidates for comparative crystallographic analyses. Finally, temperature is another parameter that should not be neglected.

We acknowledge financial support from CNES and greatly appreciate the beam time that was allocated to this project by ESRF. CC was the recipient of a CNES fellowship.

References

Brünger, A. T., Adams, P. D., Clore, G. M., DeLano, W. L., Gros, P., Grosse-Kunstleve, R. W., Jiang, J.-S., Kuszewski, J., Nilges, M., Pannu, N. S., Read, R. J., Rice, L. M., Simonson, T. & Warren, G. L. (1998). *Acta Cryst.* D**54**, 905–921.
Carter, C. W. Jr & Carter, C. W. (1979). *J. Biol. Chem.* **254**, 12219–12223.
Carter, C. W., Doublié, S. & Coleman, D. E. (1994). *J. Mol. Biol.* **238**, 346–365.
Chantalat, L., Nicholson, J. M., Lambert, S. J., Reid, A. J., Donovan, M. J., Reynolds, C. D., Wood, C. M & Baldwin, J. P. (2003). *Acta Cryst.* D**59**, 1395–1407.
Charron, C., Kadri, A., Robert, M.-C., Giegé, R. & Lorber, B. (2002). *Acta Cryst.* D**58**, 2060–2065.
Charron, C., Sauter, C., Zhu, D. W., Ng, J. D., Kern, D., Lorber, B. & Giegé, R. (2001). *J. Cryst. Growth*, **232**, 376–386.
Crosio, M. P., Janin, J. & Jullien, M. (1992). *J. Mol. Biol.* **228**, 243–251.
Cudney, B., Patel, S., Weisgraber, K., Newhouse, Y. & McPherson, A. (1994). *Acta Cryst.* D**50**, 414–423.
Ducruix, A. & Giegé, R. (1999). *Crystallization of Nucleic Acids and Proteins. A Practical Approach.* Oxford: IRL Press.
Jancarik, J. & Kim, S.-H. (1991). *J. Appl. Cryst.* **24**, 409–411.
Jones, T. A., Zou, J. Y., Cowan, S. W. & Kjeldgaard, M. (1991). *Acta Cryst.* A**47**, 110–119.
Kabsch, W. (1993). *J. Appl. Cryst.* **26**, 795–800.
Kingston, R. L., Baker, H. M. & Baker, E. N. (1994) *Acta Cryst.* D**50**, 429–440.
Ko, T.-P., Day, J., Greenwood, A. & McPherson, A. (1994). *Acta Cryst.* D**50**, 813–825.
Laskowski, R. A., MacArthur, M. W., Moss, D. S. & Thornton, J. M. (1993). *J. Appl. Cryst.* **26**, 283–291.
Lee, B. & Richards, F. M. (1971). *J. Mol. Biol.* **55**, 379–400.
Lorber, B. & Cudney, R. (2002). *J. Appl. Cryst.* **35**, 509–510.

McPherson, A. (1999). *Crystallization of Biological Macromolecules.* Cold Spring Harbor, NY, USA: Cold Spring Harbor Laboratory Press.
McPherson, A. & Weickmann, J. (1990). *J. Biomol. Struct. Dyn.* **7**, 1053–1060.
Matthews, B. W. (1968). *J. Mol. Biol.* **33**, 491–497.
Navaza, J. (1994). *Acta Cryst.* A**50**, 157–163.
Samudzi, C. T., Fivash, M. J. & Rosenberg, J. M. (1992). *J. Cryst. Growth*, **123**, 47–58.
Sauter, C., Lorber, B. & Giegé, R. (2002). *Proteins Struct. Funct. Genet.* **48**, 146–150.
Sedzik, J. & Norinder, U. (1997). *J. Appl. Cryst.* **30**, 502–506.
Segelke, B. W. (2001). *J. Cryst. Growth*, **232**, 553–562.
Stura, E. A., Satterthwait, A. C., Calvo, J. C., Kaslow, D. C. & Wilson, I. A. (1994). *Acta Cryst.* D**50**, 448–455.
Vos, A. M. de, Hatada, M., van der Wel, H., Krabbendam, H., Peerdeman, A. F. & Kim, S.-H. (1985). *Proc. Natl Acad. Sci. USA*, **82**, 1406–1409.
Wel, H. van der, van Soest, T. C. & Royers, E. C. (1975). *FEBS Lett.* **56**, 316–317.